Solid State Communications 264 (2017) 6–9

Contents lists available at ScienceDirect

Solid State Communications

journal homepage: www.elsevier.com/locate/ssc

Communication

The second peak effect and vortex pinning mechanisms in $Ba(Fe,Ni)_2As_2$ superconductors

S.R. Ghorbani[a,*], H. Arabi[a], X.L. Wang[b]

[a] Department of Physics, Faculty of Science, Ferdowsi University of Mashhad, Mashhad 9177948974, Iran
[b] Institute for Superconducting and Electronic Materials, University of Wollongong, Wollongong, NSW 2522, Australia

ARTICLE INFO

Communicated by: A.H. MacDonald

PACS numbers:
74.70.Xa
74.25.Wx
74.25.Sv

Keywords:
$BaFe_{1.9}Ni_{0.1}As_2$ single crystal
Critical current density
Flux pinning
Second peak

ABSTRACT

Vortex pinning mechanisms have been studied systematically in $BaFe_{1.9}Ni_{0.1}As_2$ single crystal as a function of temperature and magnetic field. The obtained shielding current density, J_s, showed a second peak in the intermediate magnetic field range at high temperatures. The temperature dependence of the shielding current density, $J_s(T)$, was analysed within the collective pinning model at different magnetic fields. It was found that the second peak reflects the coexistence of both δl pinning, reflecting spatial variation in the mean free path (l), and δT_c pinning, reflecting spatial variation in the superconducting critical temperature (T_c) at low temperature and low magnetic fields in $BaFe_{1.9}Ni_{0.1}As_2$ single crystal. The results clearly show that pinning mechanism effects are strongly temperature and magnetic field dependent, and the second peak effect is more powerful at higher temperatures and magnetic fields. It was also found that the magnetic field mainly controls the pinning mechanism effect.

1. Introduction

Fe-based superconductors have the highest transition temperature (T_c = 56–57 K) [1,2] among non-cuprate high-T_c layered superconductor compounds. High upper critical fields over 100 T have been reported for these superconductors [3]. This is attractive for technical applications that require not only a high upper critical field, but also where it is necessary to carrying a large supercurrent. Therefore, a high critical current density, J_c, is one of major physical requirements for superconducting materials at low, and in particular, high magnetic fields. The current-carrying ability of Fe-based superconductors at high fields and temperatures is largely determined by the flux-pinning strength and the behaviour of the vortex matter. Therefore, the determination of the intrinsic vortex pinning mechanism is a central issue from both an applied and fundamental perspectives.

At a given temperature, the critical current of a superconductor usually decreases with increasing applied magnetic field. There are several reports on an anomalous increase in the critical current at intermediate fields, however, which is denoted as a "peak or secondary peak" effect and occurs in low temperature superconductors [4], MgB_2 [5], and the cuprate high-temperature superconductors [6]. In the iron-based superconductors, the peak effect has been observed in FeAs-1111 [3,7], in FeAs-122 [8], and in $FeTe_{1-x}Se_x$ [9].

The secondary peak effect relative to the first peak near zero magnetic field is a unique feature in the field dependence of magnetic hysteresis or critical current curves, but its features vary from one compound to the next [5,10,11]. It is well known that the current-density decay behaviour is governed by the pinning mechanism. In type-II superconductors, the flux pinning is controlled by two basic pinning mechanisms [12,13]. The first is the pinning due to the randomly distributed spatial variations in the transition temperature T_c, which is called δT_c pinning [14,15]. The second pinning mechanism relates to spatial fluctuation of the charge-carrier mean free path, l, the so called δl pinning, which is mostly due to crystal lattice defects [13,16,17]. Preliminary experimental results indicate that the vortex dynamics in Fe-based superconductors may be understood through the thermally activated flux motion model based on collective vortex pinning [8,18,19], although the relationship between the secondary peak and the flux pinning mechanism has not been studied so far.

In this work, the variation of the shielding current density, J_s, with respect to applied magnetic field and temperature is discussed. At very low temperatures, the obtained results show that the J_s decreases strongly at low magnetic field in $BaFe_{1.9}Ni_{0.1}As_2$ single crystal, but after that, it becomes nearly field independent. With increasing temperature, a second peak is observed in the shielding current density in the intermediate magnetic field range. The vortex pinning mechanisms of $BaFe_{1.9}Ni_{0.1}As_2$ crystal were therefore studied systematically. The correlation between the secondary peak effect and the flux pinning

* Corresponding author.
E-mail address: sh.ghorbani@um.ac.ir (S.R. Ghorbani).

http://dx.doi.org/10.1016/j.ssc.2017.07.007
Received 13 June 2017; Received in revised form 12 July 2017; Accepted 18 July 2017
Available online 19 July 2017

mechanisms was systematically studied as a function of applied magnetic field and temperature. The results show that both the δl and δT_c pinning mechanisms coexist in the $BaFe_{1.9}Ni_{0.1}As_2$ crystal. Their contributions are strongly temperature and magnetic field dependent. It was found that, in the presence of the second peak, the contributions of both the δl and δT_c pinning mechanisms are changed.

2. Experiment

Single crystals with the nominal composition $BaFe_{1.9}Ni_{0.1}As_2$ were prepared by a self-flux method. The crystal growth details are given in Ref. [20]. The critical temperature T_c was defined as the onset temperature at which diamagnetic properties were observed. This temperature was 17.6 K. The magnetization was measured using a magnetic properties measurement system (MPMS, Quantum Design).

The J_s was obtained from the width ΔM of the magnetization loops, which were collected in different fields and temperatures using the Bean model. According to this model $J_s = 20\Delta M/Va(1-a/3b)$ for full sample penetration, where a and b are the width and the length of the sample perpendicular to the applied field, respectively, and V is the sample volume.

3. Results and discussion

Fig. 1 shows the resulting J_s versus applied field, which was perpendicular to the FeAs plane. At the temperature of 3 K, the zero field J_s value is 2.0×10^5 A/cm^2, and it only decreases to 0.8×10^5 A/cm^2 at $B = 8$ T. The weak dependence of J_s on field suggests superior J_s behaviour for the $Ba(Fe,Ni)_2As_2$ single-crystal superconductor, which is beneficial for potential applications in high magnetic fields. As can be seen in Fig. 1, the J_s decreases with increasing field up to roughly 1 T, and after that, it becomes nearly field independent at very low temperatures. With increasing temperature, a prominent broad peak or second peak at the field of B_{sp} was observed in J_s in the intermediate field range. As shown in inset of Fig. 1, the second peak position B_{sp}, where B_{sp} is the magnetic field at the second maximum of the $J_s(B)$ value for $B > 0$, moves toward lower field as the temperature rises. Assuming power law behaviour for B_{sp}, the solid curve in the inset of Fig. 1 is the best fit curve to the equation $B_{sp} = A(1\text{-}T/T^*)^{1.5}$, which was used before for $YBa_2Cu_3O_{7-\delta}$ (Y-123) superconductor [6], where A and T^* are fitting parameters. The best-fit values of A and T^* are 8.04 T and 17.4 K, respectively. T^* in the present case is equal to the critical temperature of 17.6 K. This remarkable likeness between the results obtained for both Y-123 cuprate and $BaFe_{1.9}Ni_{0.1}As_2$ superconductors might suggest that the peak effect in the two systems has the same origin.

The normalised J_s is presented in Fig. 2 as a function of the reduced

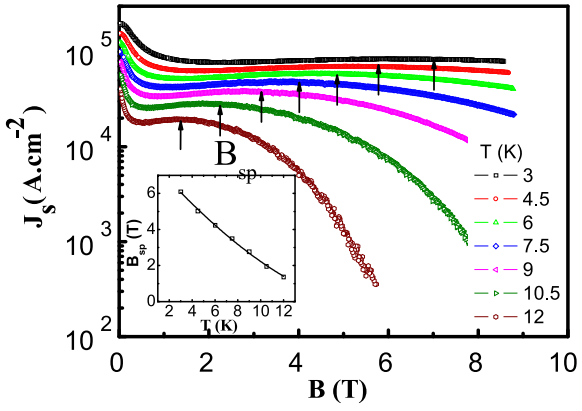

Fig. 1. J_s-field dependence for $BaFe_{1.9}Ni_{0.1}As_2$ single crystal. Inset: B_{sp} as a function of temperature. The solid curve in the inset is the best fit curve to the T dependence of the B_{sp}.

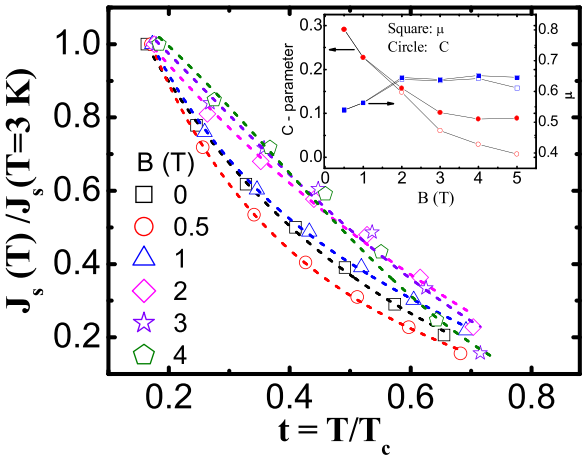

Fig. 2. Temperature dependence of the normalised measured J_s at fields of 0–4 T. The dashed lines are the theoretical curves based on the model of coexistence between the δl and δT_c pinning mechanisms. Inset: Field dependence of C and μ parameters without (open symbols) and with (solid symbols) consideration of the second peak, which will be discussed later.

temperature $t = T/T_c$ at fields of 0–4 T. In order to quantify the current densities of high-T_c superconductors in the framework of the thermally activated flux motion model and the model of collective flux pinning and creep, the expression $U(J) = U_0/\mu[(J_c/J_s)^{\mu}-1]$ for the dependence of the activation energy is proposed [12,21], where U_o and J_c are, respectively, the temperature dependent potential barrier height and the critical current density in the absence of flux creep. Therefore, U depends implicitly on temperature through the quantities U_o and J_c. μ, the glassy exponent, is a parameter that varies as a function of the vortex-vortex and vortex-pinning centre interactions. This means that this parameter has an influence on the current dependence of $U(T)$ and depends on the flux creep regime [21]. It was also found from studying the electric field vs. current density (E-J) curves that a negative μ value corresponds to plastic vortex motion, while a positive μ indicates elastic vortex motion [15]. The temperature dependence of J_s was found [22] by considering an effective attempt time, t_{eff}, for a flux segment/bundle to jump over a potential barrier and the recorded time, t_1, as:

$$J_s(T) = \frac{J_{dp}(T)}{\left\{1+\left[\mu k_B T \ln\left(\frac{t_1}{t_{eff}}\right)/U(T)\right]\right\}^{1/\mu}} \quad (1)$$

where $J_{dp}(T)$ is the depinning current density. By assuming $U(T) = U_c(0)\, g(t)$ and $J_{dp}(T) = J_c(0)J(t)$, where $U_c(0)$ and $J_c(0)$ are the corresponding values at $T = 0$ K, and $g(t)$ and $J(t)$ are, respectively, the reduced temperature, $t = T/T_c$, dependent activation energy and critical current density, the following temperature dependence for $J_s(T)$ can be obtained:

$$J_s(T) = \frac{J_c(0)J(t)}{\{1+[\mu k_B TC/g(t)]\}^{1/\mu}} \text{ with } C = \ln\left(\frac{t_1}{t_{eff}}\right)/U_c(0) \quad (2)$$

where C is a temperature independent parameter.

It was pointed out that the δl and δT_c pinning mechanisms result in different temperature dependencies of $J(t)$ and $g(t)$ as [13]:

$$J(t) = (1-t^2)^{7/6}(1+t^2)^{5/6} \quad (3)$$

$$g(t) = (1-t^2)^{1/3}(1+t^2)^{5/3} \quad (4)$$

for δT_c pinning, and

$$J(t) = (1-t^2)^{5/2}(1+t^2)^{-1/2} \quad (5)$$

$$g(t) = 1 - t^4 \quad (6)$$

for δl pinning. One can easily find from Eqs. (2), (3), and (5) that at $T =$

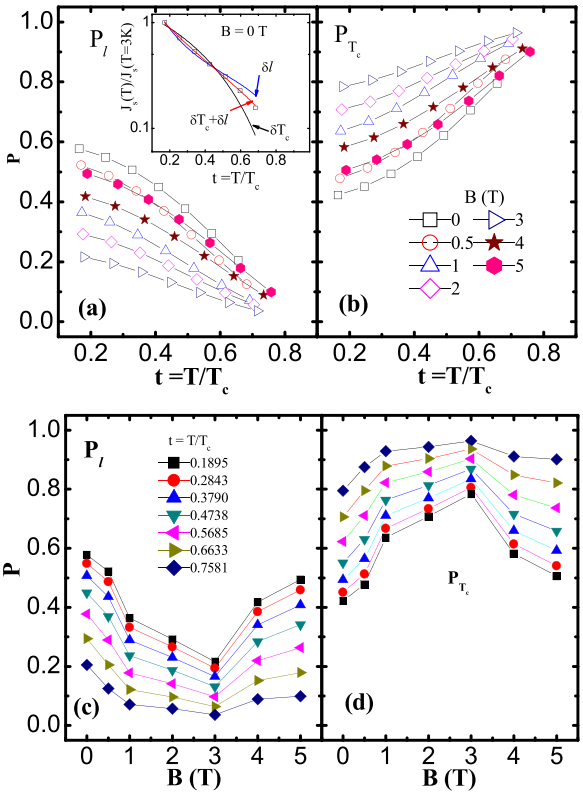

Fig. 3. (Color online) Pinning effect contributions of (a) δl and (b) δT_c pinning as functions of reduced temperature at different fields. Magnetic field dependence of (c) the δl and (d) the δT_c pinning contributions at different temperatures. Inset shows the theoretical curves obtained based on the model of the δl (blue curves) pinning mechanism, the model of the δT_c (black curves) pinning mechanism, and the coexistence of both (red curves) pinning mechanisms.

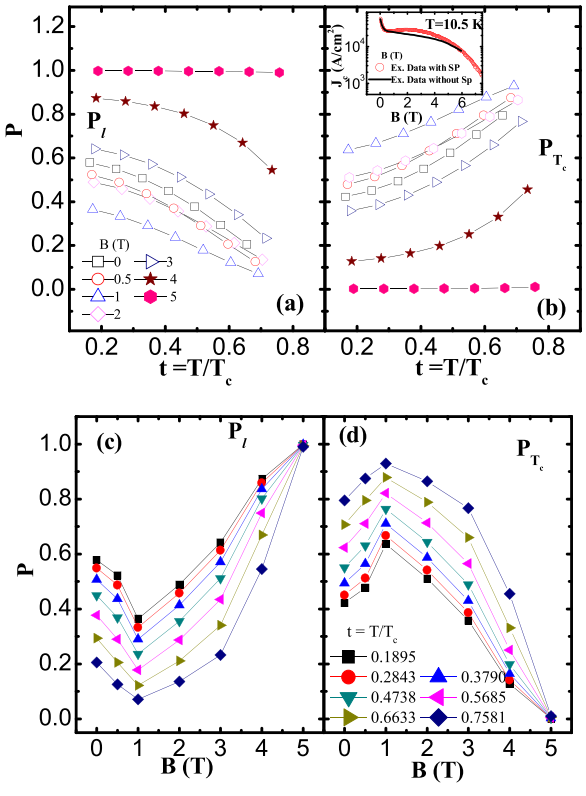

Fig. 4. Reduced temperature dependence of (a) the δl and (b) the δT_c pinning effects, and field dependence of (c) the δl and (d) the δT_c pinning effects without considering the second peak. Inset: The experimental (○ symbol) and expected (black curve) critical current density with and without considering the second peak for the temperature of T = 10.5 K.

0 K, $J_s(0) = J_c(0)$, so we can fit the J_s data with Eq. (2) by adjusting only two parameters, i.e., C and μ. The inset of Fig. 3(a) shows that the theoretical curves that were based on either the δl model or the δT_c model of pinning cannot describe the experimentally obtained J_s. As can be seen in the inset of Fig. 3(a), the real experimentally obtained curves reside in between those for the δl pinning and δT_c pinning mechanisms. This indicates that both the δl and the δT_c pinning coexist in the Fe-122 single crystal. Therefore, to investigate further the real pinning mechanism, the $J_s(T)$ data was analysed by assuming the coexistence of both the δl and the δT_c pinning mechanisms in accordance with the following expression [16]:

$$J_s(T) = P_1 J_s^{l}(T) + P_2 J_s^{T_c}(T) \quad (7)$$

where $J_s^{l}(T)$ and $J_s^{T_c}(T)$ are the expressions for the δl and the δT_c pinning, respectively. P_1 and P_2 are fitting parameters. The $J_s(T)$ data are well described by Eq. (7) in the studied range of fields, as shown by the dashed curves in Fig. 2 and the inset of Fig. 3(a). The inset of Fig. 2 shows the field dependence of both the C and μ parameters. The best-fit value of μ is 0.6 ± 0.05, which is intermediate between the single vortex value, μ = 1/7, and the small bundle value, μ = 3/2, for $BaFe_{1.9}Ni_{0.1}As_2$ crystal. The value of μ is positive, which indicates elastic vortex motion, and is in rough agreement with μ = 0.45 and 0.38 for $Ba(Fe_{1-x}Co_x)As_2$ [23] and $Ba_{0.72}K_{0.28}Fe_2As_2$ crystal [24], respectively. The field dependence of the C parameter is shown in the inset of Fig. 2, where C decreases with increasing field. The field dependence of the C parameter may be introduced through both the $\ln(t/t_{eff})$ term and the temperature independent pinning potential U_0. For the $BaFe_{1.9}Ni_{0.1}As_2$ crystal, the U_0 is dependent on field in the field range studied here, and it scales as $B^{-1.17}$ for $B > 1$ T [25]. It was found [26] that $\ln(t/t_{eff}) = \ln[2v_0B/a(dB/dt)]$, where v_0 is the attempt velocity, which is expected to be field dependent, since single-vortex hopping occurs at low fields,

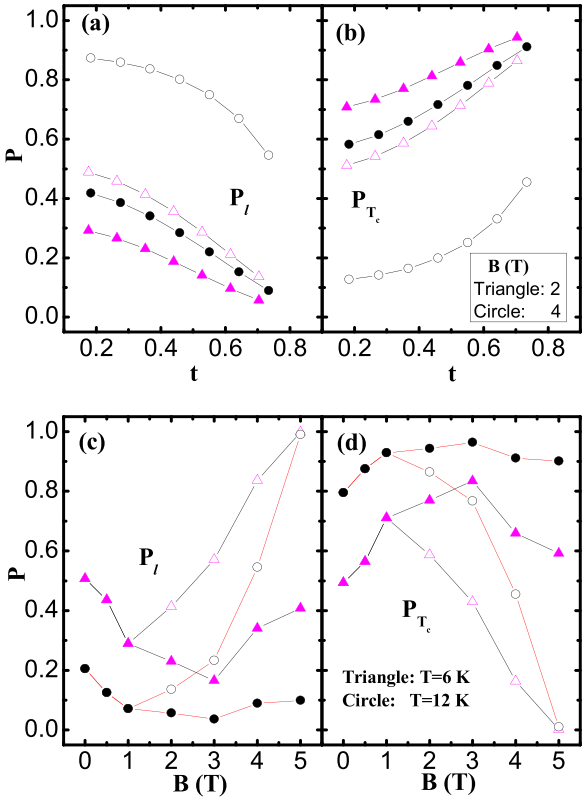

Fig. 5. Comparison between (a) the δl and (b) the δT_c pinning effects with (solid symbols) and without (open symbols) consideration of the second peak as functions of reduced temperature and (c), (d) as functions of field, respectively.

while flux-bundle motion is expected at high fields. a is the lateral dimension of the sample, and dB/dt is the sweep rate of the magnetic field B.

In order to obtain the contributions of the δl and the δT_c pinning mechanisms, the P parameter was defined as $P_l = P_1 J_s^l(T)/J_s(T)$ and $P_{T_c} = P_2 J_s^{T_c}(T)/J_s(T)$ with $P_l + P_{T_c} = 1$ [16]. These parameters represent the δl and the δT_c pinning effects, respectively. Fig. 3 shows both types of pinning effect contributions for $BaFe_{1.9}Ni_{0.1}As_2$ single crystal. As can be seen in Fig. 3, the pinning mechanism strongly depends on both the reduced temperature, $t = T/T_c$, and the field. At reduced temperatures below 0.4, the two pinning mechanisms have roughly equal effects, while above this reduced temperature, δT_c pinning is dominant. The trends in the results show that when the temperature is far below T_c, the T_c fluctuation disappears, and the δl pinning is dominant. For further explaining the influence of field on the pinning effects, the field dependence of both the δl and the δT_c pinning mechanisms are shown in Fig. 3(c) and (d). Both δl and δT_c pinning coexist at the fields studied here. The δl pinning decreases with increasing field up to $B = 3$ T and with increasing reduced temperature. But for $B > 3$ T, the trend in the pinning mechanism changes: the δl pinning effect starts to increase with magnetic field, while the δT_c pinning shows the opposite trend. This result implies that the mean free path l and the critical temperature T_c fluctuation depend on magnetic field through the disorder parameter in the framework of the collective flux pinning and creep model [12]. The possible reason for the changing trend in the pinning effect also may due to the transition from the single vortex regime to the small bundle or the large bundle creep regime with increasing the magnetic field and results in differences in the disorder parameter. Thus, further study is needed in order to obtain the relationship between both the δl and the δT_c pinning behaviour and magnetic field.

As mentioned in the introduction section, the relationship between the secondary peak effect and the flux pinning mechanism of iron-based superconductors has not been reported so far. The starting point for the influence of the secondary peak effect on the flux pinning mechanism is the question of how this effect can be obtained. To answer this question, the influence of the peak effect on the flux pinning mechanisms was systematically studied as a function of the field at different temperatures, using Eqs. (2) and (7) without consideration of the second peak. In many of the Fe-based superconductors such as $Ba_{0.72}K_{0.28}Fe_2As_2$ crystals [24], the second peak did not appear in $J_s(B)$ curves. Therefore, the J_s behaviour without consideration of the second peak is similar to the $J_s(B)$ curves for $Ba_{0.72}K_{0.28}Fe_2As_2$ crystals, and it is expected to be the same as the black curve in the inset of Fig. 4 for the temperature of $T = 10.5$ K. The experimental values for the J_s were also added to the inset of Fig. 4 for comparison of the J_s behaviour with and without considering the second peak. The results for the C parameter and the μ parameter with consideration of the second peak have been added to the inset of Fig. 2 for comparison. As can be seen in inset of Fig. 2, the μ parameter does not even show a rough dependence on the second peak, while the C parameter increases with increasing field at higher fields or in the flux-bundle motion region. The temperature and field dependence of both the δl and the δT_c pinning mechanism results without considering the second peak are shown in Fig. 4.

As can be seen in Fig. 4, the pinning mechanism dependences on temperature and field are stronger than those shown in Fig. 3. At temperatures below 4.5 K and $B \leq 3$ T, the two pinning mechanisms coexist, and they have roughly equal effects, while above this temperature, δT_c pinning is dominant. The δl pinning is dominant at high fields, for $B \geq 5$ T and high temperatures, while the δT_c pinning is suppressed completely, and therefore, the δl pinning is the only effective pinning mechanism, which is supported by reported results for $Ba_{0.72}K_{0.28}Fe_2As_2$ crystal [24].

In order to reach a further understanding of the effects of the second peak on the pinning mechanism, the results from Figs. 3 and 4 for both the δl and the δT_c pinning effects are replotted in Fig. 5 for comparison. The results in Fig. 5(a) and (b) show that the δl pinning effect is decreased in the presence of the second peak, but the δT_c pinning effect is increased, with the proportions dependent on the magnetic field. At $B = 4$ and 5 T, the value of the δl pinning contribution decreases by about 50% and 90%, respectively, while the value of the δT_c pinning contribution shows a different trend. Therefore, these results clearly show that the second peak effect has a greater influence at higher temperatures and magnetic fields. A crossover transition at magnetic field of 1 T, where the trend in the pinning mechanism changes with the appearance of the second peak, was found (Fig. 5(c, d)). This transition occurs between the single vortex regime and the collective flux-creep regime with slower relaxation. For temperatures close to T_c and $B \geq 1$ T, the T_c fluctuation increases, and therefore, the δl pinning is suppressed. When the temperature is far below T_c, the T_c fluctuation disappears, and the δl pinning may be the dominant mechanism.

In conclusion, from the temperature dependence of the J_s within the collective pinning model at different fields, it was found that the second peak is correlated with the coexistence of both the δl pinning and the δT_c pinning effect at low temperature and low fields in $BaFe_{1.9}Ni_{0.1}As_2$ single crystal. The results clearly show that the correlation with the second peak is stronger at higher temperatures and fields.

Acknowledgements

This work was supported by the Ferdowsi University of Mashhad, Iran (Grant no. 2/43489). Dr. T. Silver's critical reading of this paper is greatly appreciated.

References

[1] Y. Kamihara, T. Watanabe, M. Hirano, H. Hosono, J. Am. Chem. Soc. 130 (2008) 3296.
[2] P. Cheng, B. Shen, G. Mu, X.Y. Zhu, F. Han, B. Zeng, H.H. Wen, Eur. Phys. Lett. 85 (2009) 67003.
[3] C. Senatore, R. Flükiger, M. Cantoni, G. Wu, R.H. Liu, X.H. Chen, Phys. Rev. B 78 (2008) 054514.
[4] W.D. Sorbo, Rev. Mod. Phys. 36 (1964) 90.
[5] M. Pissas, S. Lee, A. Yamamoto, S. Tajima, Phys. Rev. Lett. 89 (2002) 097002.
[6] L. Klein, E.R. Yacoby, Y. Yeshurun, A. Erb, G. Müller-Vogt, V. Breit, H. Wühl, Phys. Rev. B 49 (1994) 4403.
[7] R. Prozorov, M.E. Tillman, E.D. Mun, P.C. Canfield, New J. Phys. 11 (2009) 035004.
[8] H. Yang, H. Luo, Z. Wang, H.H. Wen, Appl. Phys. Lett. 93 (2008) 142506.
[9] P. Das, Ajay D. Thakur, Anil K. Yadav, C.V. Tomy, M.R. Lees, G. Balakrishnan, S. Ramakrishnan, A.K. Grover, Phys. Rev. B 84 (2011) 214526.
[10] M. Daumling, J.M. Senntjens, D.C. Larbalestier, Nature 346 (1980) 332.
[11] Y. Abulafia, A. Shaulov, Y. Wolfus, R. Prozorov, L. Burlachkov, Y. Yeshurun, D. Majer, E. Zeldov, H. Wuhl, V.B. Geshkenbein, V.M. Vinokur, Phys. Rev. Lett. 77 (1996) 1596.
[12] G. Blatter, M.V. Feigelman, V.B. Geshkenbein, A.I. Larkin, V.M. Vinokur, Rev. Mod. Phys. 66 (1994) 1125.
[13] R. Griessen, H.H. Wen, A.J.J. van Dalen, B. Dam, J. Rector, H.G. Schnack, S. Libbrecht, E. Osquiguil, Y. Bruynseraede, Phys. Rev. Lett. 72 (1994) 1910.
[14] M.J. Qin, X.L. Wang, H.K. Liu, S.X. Dou, Phys. Rev. B 65 (2002) 132508.
[15] H.H. Wen, Z.X. Zhao, S.L. Yan, L. Fang, M. He, Phys. C 312 (1999) 274.
[16] S.R. Ghorbani, X.L. Wang, S.X. Dou, Sung-IK Lee, M.S.A. Hossain, Phys. Rev. B 78 (2008) 184502.
[17] C. Dong, H. Lin, H. Huang, C. Yao, X. Zhang, D. Wang, Q. Zhang, Y. Ma, S. Awaji, K. Watanabe, J. Appl. Phys. 119 (2016) 143906.
[18] R. Prozorov, M.A. Tanatar, P. Prommapan, R.T. Gordon, N. Ni, S.L. Bud'ko, P.C. Canfield, Phys. C 469 (2009) 667.
[19] X.L. Wang, S.R. Ghorbani, S.I. Lee, S.X. Dou, C.T. Lin, T.H. Johansen, K.H. Müller, Z.X. Cheng, G. Peleckis, M. Shabazi, A.J. Qviller, V.V. Yurchenko, G.L. Sun, D.L. Sun, Phys. Rev. B 82 (2010) 024525.
[20] A.S. Sefat, R. Jin, M.A. McGuire, B.C. Sales, D.J. Singh, D. Mandrus, Phys. Rev. Lett. 101 (2008) 117004.
[21] M.V. Feigel'man, V.B. Geshkenbein, A.I. Larkin, V.M. Vinokur, Phys. Rev. Lett. 63 (1989) 2303.
[22] J.R. Thompson, Yang Ren Sun, L. Civale, A.P. Malozemoff, M.W. McElfresh, A.D. Marwick, F. Holtzberg, Phys. Rev. B 47 (1993) 14440.
[23] B. Shen, Peng Cheng, Zhaosheng Wang, Lei Fang, Cong Ren, Lei Shan, Hai-Hu Wen, Phys. Rev. B 81 (2010) 014503.
[24] S.R. Ghorbani, X.L. Wang, M. Shahbazi, S.X. Dou, C.T. Lin, Appl. Phys. Lett. 100 (2012) 212601.
[25] M. Shahbazi, X.L. Wang, S.R. Ghorbani, M. Ionescu, O.V. Shcherbakova, F.S. Wells, A.V. Pan, S.X. Dou, K.Y. Choi, Supercond. Sci. Technol. 26 (2013) 095014.
[26] H.H. Wen, H.G. Schnack, R. Griessen, B. Dam, J. Rector, Phys. C 261 (1995) 353.